Fish & Shellfish Immunology 47 (2015) 485–499

Contents lists available at ScienceDirect

Fish & Shellfish Immunology

journal homepage: www.elsevier.com/locate/fsi

Full length article

A novel innexin2 forming membrane hemichannel exhibits immune responses and cell apoptosis in *Scylla paramamosain*

Shu-Ping Wang [a, 1], Fang-Yi Chen [a, b, c, 1], Li-Xia Dong [a], Ya-Qun Zhang [a], Hui-Yun Chen [a, b, c], Kun Qiao [a], Ke-Jian Wang [a, b, c, *]

[a] State Key Laboratory of Marine Environmental Science, College of Ocean & Earth Science, Xiamen University, Xiamen, Fujian, PR China
[b] Fujian Collaborative Innovation Center for Exploitation and Utilization of Marine Biological Resources, Xiamen University, Xiamen, Fujian, PR China
[c] Fujian Engineering Laboratory of Marine Bioproducts and Technology, Xiamen University, Xiamen, Fujian, PR China

ARTICLE INFO

Article history:
Received 22 June 2015
Received in revised form
6 September 2015
Accepted 14 September 2015
Available online 15 September 2015

Keywords:
Scylla paramamosain
Innexin
Hemichannel
Immune response
Apoptosis

ABSTRACT

Innexins are a class of transmembrane proteins that are important for embryonic development, morphogenesis and electrical synapse formation. In the present study, a novel innexin2 gene from *Scylla paramamosain* was named Sp-inx2 and characterized. The complete cDNA and genomic DNA sequences of Sp-inx2 were revealed. Sp-inx2 mRNA transcripts were distributed in various tissues of *S. paramamosain* and were most abundant in the hemocytes. The Sp-inx2 was significantly upregulated in hemocyte, gill and hepatopancreas tissues with the challenge of either *Vibrio alginolyticus*, *Vibrio parahaemolyticus* or lipopolysaccharides (LPSs) when analyzed at 3 and 6 h using quantitative real-time PCR, suggesting that it could activate an immune response against the challenge of LPSs or *Vibrio* species. Using the chemical inhibitors carbenoxolone and probenecid, the absorption of the fluorescent dye Lucifer yellow decreased in the primary cultured hemocytes of crabs, thus confirming that hemichannels composed of Sp-inx2 existed in the crab hemocytes. With LPS stimulation, the level of mRNA transcripts and protein expression of Sp-inx2 in the same cultured hemocytes gradually increased from 6 to 48 h, while the activity of hemichannels was down-regulated at 6 and 12 h, demonstrating that LPSs could modulate the absorption activity of hemichannels in addition to its upregulation of Sp-inx2 gene expression. Furthermore, the dye uptake rate in HeLa cells in which Sp-inx2 was ectopically expressed increased dramatically but the increase was significantly down-regulated with the addition of 50 μg mL^{-1} LPS, suggesting that the LPS stimulation could effectively reduce the activity of hemichannels. Interestingly, with the ectopic expression of Sp-inx2 in HeLa and EPC cells, apoptosis spontaneously occurred in both cultured cell lines when detected using TUNEL assay. In summary, a new Sp-inx2 gene was first characterized in a marine animal *S. paramamosain* and it had a function associated with immune response and cell apoptosis.

1. Introduction

Gap junctions (GJs) are found in most cells and tissues in all metazoan organisms and exert a function to promote intercellular communication [1,2]. GJs are composed of a pair of six polymer hemichannels. Each hemichannel consists of six connexin (in vertebrates) or innexin (in invertebrates) subunits. Hemichannels of adjacent cells interact with each other, and form a functional dodecameric GJ channel directly linking the cytoplasm of neighboring cells [3].

In vertebrates, there are not only connexins but also pannexins. Pannexins (not connexins) are homologous to invertebrate innexin proteins, and they all share a similar protein topology. Evolutionarily speaking, pannexins might be the chordate members of the innexin superfamily. Innexins in invertebrates might have a dual role, possibly providing the partial functions of both connexins and pannexins. Innexin, connexin and pannexin all have four transmembrane regions, two extracellular cycles, one intracellular cycle and intracellular N- and C-terminal tails. At least 20 connexin genes and three pannexin genes have been identified so far, likely encoding GJ proteins or hemichannel proteins in mice and humans

* Corresponding author. State Key Laboratory of Marine Environmental Science, College of Ocean & Earth Science, Xiamen University, Xiamen, Fujian, PR China.
E-mail address: wkjian@xmu.edu.cn (K.-J. Wang).
[1] These authors made equal contributions.

http://dx.doi.org/10.1016/j.fsi.2015.09.028
1050-4648/

[2]. Multiple members of the innexin gene family are also found in invertebrates, and at least eight innexin genes are identified in *Drosophila melanogaster* [4], 25 in *Caenorhabditis elegans* [5], and 21 in the annelid *Hirudo verbana* [6]. In crustaceans, there are six innexin members which have been identified in the crab *Cancer borealis* [7]. However, there is no research on innexins in *Scylla paramamosain*.

The functions of connexins have been extensively studied, especially in embryogenesis, neurophysiology and endocrinology, however, much less is known about the function of the innexin/pannexin superfamily [8]. Some studies report that innexins are important for embryonic development, and morphogenetic and physiological regulation in invertebrates [9–11].

Previous studies reveal that innexins function mainly by forming GJs or hemichannels [12]. Dm-Inx2 GJs mediate intercellular transfer of GDP-L-fucose, a substrate for O-fucose modification, in the wing imaginal disc [11]. GJs are relatively non-selective in comparison to ligand-gated or voltage-gated channels and allow ions and small molecules such as cAMP to pass through, thus enabling electrical and metabolic signaling [8]. Some of the innexins in the *C. elegans* reproductive system do not create GJs at all, perhaps in favor of forming functional innexons which are called hemichannels [5]. The hemichannel is made of single (homomeric) or multiple (heteromeric) protein isotypes. It is possible that this hemichannel can help one cell dock with the adjacent cells under some circumstances in order to communicate with other cells. The channel activity might be very sensitive to various stimuli, such as the change of electrical potential inside and outside cells, the change of intracellular Ca^{2+} level, phosphorylation or dephosphorylation of innexin protein, immune response, and so on [13,14].

Hemichannels consisting of innexin/pannexin proteins can also regulate apoptosis. Previous studies show that insect innexons play a role in promoting apoptosis and inactivating the PI3K/Akt signaling pathway, a key cell survival pathway [15]. Moreover, the hemichannel can also participate in the process after the occurrence of apoptosis. Caspase-3 activation shears the C-termini of the pannexin1 protein, leading to the opening of the pannexin1 channel and increased ATP release [16]. This ATP release can induce phagocytes to swallow and digest the apoptotic cells and its components. In addition, gap–junction proteins act as tumor suppressors but the mechanism of action remains unclear [12].

It is noteworthy that the study on innexins is focused mainly on the fly *D. melanogaster* or the nematode *C. elegans* owing to their clear genetic background and advanced molecular techniques, whereas the relevant transmembrane proteins that function as barriers against pathogenic microorganisms in *S. paramamosain* have been less well reported. In our previous study, a novel transmembrane protein Sp-inx2 is identified by screening the suppression subtractive hybridization (SSH) cDNA library constructed in hemocytes of the mud crab *S. paramamosain* challenged with lipopolysaccharides (LPSs) [17]. This type of transmembrane protein, which was first found in *S. paramamosain*, greatly attracted us to further characterize it and evaluate its biological function. The present study was aimed to characterize the Sp-inx2 and further reveal its potential functions. The full length of the Sp-inx2 cDNA and the genomic DNA sequence were determined, and the tissue distribution plus expression patterns of Sp-inx2 in various tissues were also analyzed. Furthermore, the hemichannels in the hemocytes of *S. paramamosain* were elucidated. Considering that this channel protein itself or the signaling transduction pathways may be influenced by pathogen invasion and the hemichannel composed of Sp-inx2 may have a role involving apoptosis, we investigated the interaction between Sp-inx2 signaling, immune response and apoptosis. To our knowledge, this is the first characterization of the innexin2 gene in *S. paramamosain* and this work would much facilitate our understanding of the functional role of innexin2 in invertebrates.

2. Materials and methods

2.1. Experimental animals and hemocyte collection

Live healthy female *S. paramamosain* (with average body weight 300 ± 50 g) were purchased from a local commercial crab farm in Xiamen, China, and acclimated in seawater aquaria for one week before experiments were carried out. The haemolymph samples were prepared as previously described [17]. Briefly, 2 mL haemolymph was collected into an equal volume of anti-coagulant solution (NaCl 450 mM, glucose 100 mM, citric acid 26 mM, trisodium citrate 30 mM, EDTA 10 mM, pH 4.6) followed by centrifugation for 10 min at 4 °C, and 800 × g. The resulting hemocyte pellets were used for total RNA isolation.

2.2. Cloning of the full-length cDNA and genomic DNA sequences of Sp-inx2

Total RNA was extracted from hemocytes using TRIzol reagent (Qiagen) following the manufacturer's instructions, and treated with RQ1 RNase-free DNase (Promega) to remove the contaminated DNA. The integrity of the RNA was assessed using electrophoresis on a 1.2% formaldehyde-denatured agarose gel and visualized with ethidium bromide staining. The quantity of RNA was determined by OD260/280 measurement using a NanoDrop 2000 UV/Vis spectrophotometer (Thermo Fisher Scientific). To obtain the full-length cDNA of the Sp-inx2 gene, rapid amplification of the cDNA ends (RACE) was carried out using a SMART RACE cDNA amplification kit following the manufacturer's instructions (Clontech). Specific primers were designed based on the partial cDNA sequence obtained from an SSH cDNA library [17] (Table 1). The amplification reaction and polymerase chain reaction (PCR) temperature profiles were: 1 cycle of 94° C/5 min; 35 cycles of 94° C/30 s, 55° C/30 s, 72° C/90 s; and 7 min at 72 °C for the final extension. PCR products were gel-purified and cloned into the pMD18-T simple vector (Takara), then transformed into *Escherichia coli* DH5α competent cells. Potentially positive recombinant clones were identified using colony PCR. Positive recombinants were then selected for sequencing.

To analyze the Sp-inx2 genomic DNA organization, DNA was isolated from *S. paramamosain* muscle using a genomic DNA extraction kit (Takara). Based on the Sp-inx2 full-length cDNA

Table 1
Sequences of primers used in this study.

Primer	Sequence (5′-3′)
GSP 1	5′- CGCCCTTGAACTTCTTGC -3′
GSP2	5′- CAGCAGCATCTTCCTCACG- 3′
SMARTIIA Oligo	5′-AAGCAGTGGTATCAACGCAGAGTACGCGGG-3′
5′-CDS	5′- (T)25VN-3′
Genomic F1	5′-ATGTCGGACGTTTTCTCAGGTATCA- 3′
Genomic R1	5′-AACGAAGTTGAACATCTCGCAGGC- 3′
Genomic F2	5′-AAGGCGGCAAGGTGAAAATGC-3′
Genomic R2	5′-ATCATCCACGCCCTTGAACTTCTTG -3′
Sp-inx2CTF	5′-GCGCCATGGGCCTCACCCCCTCTGTGGCCGTGGATC-3′
Sp-inx2 CTR	5′- GGGCTCGAGATCATCCACGCCCTTGAACTTCTTG-3′
Innexin 2-q-F	5′ -ATGAGCAGCGGGTTGTG -3′
Innexin 2-q-R	5′ -TGCCTGGGTGAGCAGTTTCC -3′
β-actin F	5′ -GCCCTTCCTCACGCTATCCT- 3′
β-actin R	5′- GCGGCAGTGGTCATCTCCT -3′
pCMV-HA-inx2-F	5′- CGGAATTCCATCGGACGTTTTCTCAGGTATCA -3′
pCMV-HA-inx2-R	5′-ATAAGAATGCGGCCGCCTAATCATCCACGCCCTTGAACT-3

sequence obtained, specific primers Genomic F1, Genomic R1, Genomic F2 and Genomic R2 (listed in Table 1) were designed. The entire Sp-inx2 DNA sequence was amplified using PCR and sequenced. The amplification reaction and PCR temperature profiles were: 1 cycle of 94° C/5 min; 35 cycles of 98° C/10 s, 68 °C anneal and extension/8 min; and 1 cycle of 72° C/10 min. The PCR products were sequenced as described above.

2.3. Phylogenetic analysis of Sp-inx2

Multiple sequence alignment was carried out using innexin2 sequences of representative invertebrates, or pannexin2 sequences of several vertebrates from GenBank using DNAMAN software. A phylogenetic tree of different innexin2/pannexin2 proteins was constructed using the neighbor-joining method with Molecular Evolution Genetics Analyses software version 6.0.

2.4. Polyclonal antibody preparation

The sequence encoding carboxyl terminal amino acids of Sp-inx2 were amplified using the gene-specific primers: Sp-inx2 CTF and Sp-inx2 CTR (listed in Table 1). An *NcoI* site was added to the 5′ end of Sp-inx2 CTF and an *XhoI* site was added to the 5′ end of Sp-inx2 CTR before the stop codon. The PCR products were digested completely using the restriction enzymes, *NcoI* and *XhoI*, and then ligated into a pET-28a expression vector. The pET-28a/Sp-inx2 carboxyl terminal recombinant plasmid was transformed into *E. coli* strain BL21 (DE3) (TransGen Biotech), and protein expression was induced using isopropyl β-D-1-thiogalactopyranoside (MDBio). The recombinant product was purified through polyacrylamide gel. The purified recombinant protein was used as an antigen to immunize BALB/c mice for more than one month until the level of antibody in their serum reached the titer required for the experiment. The immunization serum was purified using Nab™ Spin Kit, 1 mL for Antibody Purification (Thermo Scientific) following the manufacturer's instructions. The titer, purity and specificity of the purified anti-Sp-inx2 antibody were analyzed using an ultraviolet spectrophotometer, ELISA, SDS-PAGE and immune-blotting.

2.5. Transcripts and protein distribution of Sp-inx2 in various tissues

To investigate tissue gene expression patterns, equal amounts of tissues from healthy crabs were collected and used for tissue-specific expression analysis. The hemocytes were collected as described above, and other tissues including eyestalk, muscle, gills, spermatheca, stomach, hepatopancreas, oviduct, midgut gland, heart, brain, thoracic ganglion mass and ovary were also dissected and prepared for total RNA isolation as described above. One microgramme of total RNA was reverse transcribed using a PrimeScript RT reagent Kit (TaKaRa) following the manufacturer's protocol. Quantitative real-time PCR (qPCR) was performed within a reaction mixture of 20 μL containing 5 ng of total transcribed cDNA, 10 μL Power SYBR Green PCR Master Mix (Applied Biosystems, UK, (ABI)) following the manufacturer's specifications in a 7500 Real-Time PCR system (ABI). The procedure was: 50 °C for 2 min, 95 °C for 10 min, followed by 40 cycles of 95 °C for 15 s, and 60 °C for 1 min. Amplifications were repeated in triplicate. DEPC water for the replacement of template was used as the negative control.

For western blotting, the hemocytes of *S. paramamosain* were collected as described above, dissolved in RIPA buffer (Beyotime) and homogenized using an electric homogenizer (IKA). The tissues including eyestalk, gills, midgut gland, heart, stomach, muscle, spermatheca, oviduct and ovary were separately ground into powder in liquid nitrogen and lysed with RIPA. After centrifugation at 12000 g at 4 °C, the protein concentration in the supernatant was determined using the BCA method (Thermo Scientific Pierce BCA Protein Assay Kit). Proteins were separated using SDS-PAGE. Protein bands were visualized with Western blotting using mouse anti-Sp-inx2 IgG (1:800 dilution) as the primary antibody and Goat Anti-Mouse IgG as the secondary antibody (1:5000 dilution). β-actin antibody (Santa Cruz Biotechnology) was used as the internal reference. The PVDF membrane (BIO-RAD) was incubated with Immobilion™ Western HRP Substrate Peroxide Solution/Western HRP Substrate Luminol Reagent mixture (Millipore) for several minutes. Positive signals of individual blots were visualized using the film developing method.

2.6. The mRNA expression profile of Sp-inx2 against the challenge of *V. alginolyticus*, *V. parahaemolyticus* and LPSs

For the bacterial challenge experiments, crabs were randomly divided into challenge and control group. Both *Vibrio alginolyticus* (CGMCC 1.1833) and *Vibrio parahaemolyticus* (CGMCC 1.1997) were cultured in LB-medium on a rotary shaker at 200 rpm, 37 °C, and harvested in the logarithmic phase of growth as monitored using optical density assay. The final concentration of bacteria was verified by serial dilutions. *V. alginolyticus* and *V. parahaemolyticus* were washed, resuspended and diluted to the appropriate concentration in sterile modified crab saline solution (NaCl 496 mM, KCl 9.52 mM, $MgSO_4$ 12.8 mM, $CaCl_2$ 16.2 mM, $MgCl_2$ 0.84 mM, $NaHCO_3$ 5.95 mM, HEPES 20 mM, PH 7.4). 30 crabs were challenged by injection of *V. alginolyticus* or *V. parahaemolyticus* (2×10^7 CFU mL^{-1} in 100 μL sterile saline solution) and 30 injected with an equal volume of sterile saline solution were used as the control. LPSs purified from *E. coli* serotype O55:B5 (L2880, Sigma) were dissolved with sterile saline solution to 5 mg mL^{-1} in stock for animal injection. For the gene expression study, 30 crabs were injected with a dose of 0.5 mg kg^{-1} LPS and 30 were injected with an equal volume of sterile saline solution as controls. Meanwhile, five normal crabs were reared in an individual tank as a normal control group in both *Vibrio* species and LPS challenge experiments.

At 3, 6, 12, 24, 48, or 96 h post injection, hemocyte, hepatopancreas and gill tissues were collected and preserved at −80 °C. RNA extraction and qPCR were as described previously.

2.7. Primary culture of *S. paramamosain* hemocytes and LPS stimulation

The haemolymph was collected and mixed with anti-coagulant agent in a 1:5 volume ratio, followed by centrifugation for 3 min at 500 × g. The supernatant was discarded, new anticoagulants were added to wash the cells and the mixture was centrifuged again. After most of the supernatant was removed, Leibovitz's L15 medium (Thermo) with 10% fetal calf serum (FBS, Gibco), 1% antibiotics (10000 units mL^{-1} penicillin and 10000 μg mL^{-1} streptomycin, Thermo) and 0.2 M NaCl was added. 100 μL hemocytes were inoculated into each well of 96-well cell culture plates. The cell number in each well was about 1×10^5. LPSs from *E. coli* were dissolved in the cell culture medium to a concentration of 1.2 mg mL^{-1} as the stock solution. The hemocytes were stimulated by LPSs with a final concentration of 100 or 200 μg mL^{-1}. For RNA extraction and protein extraction, hemocytes from every 12 or 4 wells were used as one sample. Each sample was repeated three times.

2.8. Culture of HeLa and epithelioma papulosum cyprinid (EPC) cells, plasmid construct and transfection

HeLa cells were routinely maintained in DMEM/high glucose culture (Thermo) with 10% FBS and 1% penicillin-streptomycin-liquid (100 ×, Thermo) at 37 °C in a humidified incubator with 5% CO_2. EPC cells were cultured in Leibovitz's L15 medium (Thermo) with 10% FBS and 1% penicillin-streptomycin-liquid at 26 °C.

To construct an Sp-inx2 expression plasmid for transfection experiments, the coding region of Sp-inx2 cDNA was amplified using PCR with pCMV-HA-inx2-F and pCMV-HA-inx2-R primers (as shown in Table 1) and PfuUltra II fusion HS DNA polymerase (Stratagene) using the full-length Sp-inx2 cDNA plasmid as the template. The PCR products were purified, digested and cloned into a pCMV-HA expression vector (Clontech) containing a hemagglutinin epitope at the N-terminus. The correct sequence of the recombinant plasmid was confirmed with DNA sequencing. Large-scale plasmid DNAs were prepared using a HiSpeed Plasmid Midi kit (Qiagen). Transfection was conducted using Lipofectamine 2000 transfection reagent (Invitrogen) following the manufacturer's recommendation.

2.9. Immunofluorescence of HeLa cells and hemocytes

HeLa cells were inoculated onto cover slips and cultured in a 24-well plate overnight. Meanwhile, the crab hemocytes were also prepared and cultured in cell culture plates overnight. Both cells were separately fixed with 4% paraformaldehyde for 30 min. The treated hemocytes were collected into centrifuge tubes and centrifuged at 500 × g for 3 min, rinsed with PBS, and attached onto glass slides at 4 °C for 40 min.

After the cells were washed twice with PBS, 10% goat serum (Life Technologies) was added to block the sample and samples were maintained at room temperature for 1 h. They were then incubated with mouse polyclonal anti-Sp-inx2 antibody (1:500 dilution) for 1 h. The sections were then incubated with the second antibody, the Dylight 649 conjugate of Goat Anti-Mouse IgG (H + L) (1:1000 dilution) (LiankeBio), for 45 min. DAPI (0.5 μg mL^{-1}) was used to stain cell nuclei. Samples were analyzed using confocal laser scanning microscopy (Zeiss).

2.10. Dye uptake assays

Dye uptake assays were performed to determine hemichannel activity using the fluorescent dye Lucifer yellow (LY) as described previously [18]. LY (dilisium salt, 4 mg mL^{-1}, Sigma) was added to the medium to a final concentration of 200 μg mL^{-1}. The LY dyes rapidly transfer into the cells when the channels are functionally open. The dye uptake rate can be reduced when the channel activities are inhibited. Pharmacological inhibition of hemichannel activity was tested by treating cells with carbenoxolone (CBX; Sigma) at concentrations of 10, 20 or 30 μM, or probenecid (Sigma) at concentrations of 0.5, 1 or 2 mM. After stimulation by LPSs or CBX for 2 h, or probenecid for 0.5 h, cells were incubated in LY with gentle rocking at room temperature for 4 h. Cells were then washed three times with PBS, and fixed for 30 min in 4% paraformaldehyde. After the nuclei were labeled with Hoechst (10 μg mL^{-1}) (Sigma), the absorbed cells were sealed in glass slides, and analyzed using an iCys research imaging cytometer (CompuCyte) and confocal laser scanning microscopy.

2.11. TUNEL assay

EPC cells and HeLa cells were cultured and fixed as described above. After the cells were cultured on the slide, a method based on TdT-mediated dUTP nick end labeling (TUNEL) was used to detect apoptotic cells. Cell apoptosis analysis was performed using in situ cell death detection kit (Roche). After the TUNEL reaction, samples were counterstained with DAPI (0.5 μg mL^{-1}) and then directly analyzed by iCys research imaging and confocal laser scanning microscopy.

2.12. Statistical analysis

Data are presented as mean ± SD. Statistical analysis was performed using Student's t-test for comparison between two groups. Multiple group comparison was conducted using one-way ANOVA followed by Duncan's analysis using SPSS software version 16.0. Differences were considered significant when $p < 0.05$ or $p < 0.01$.

3. Results

3.1. Characterization of Sp-inx2 cDNA and protein sequence

A partial 924-bp nucleotide sequence encoding a protein homologous to other known innexin2 was identified in the hemocyte SSH cDNA library of *S. paramamosain* stimulated with LPSs [17]. Using 5′ RACE, the full-length cDNA sequence of Sp-inx2 (designated as FJ774668.1, GenBank) was obtained. The Sp-inx2 full-length cDNA was 1846 bp, containing a 97 bp 5′-untranslated region (UTR), a 669 bp 3′-UTR, and an ORF of 1080 bp encoding 359 amino acids with a deduced molecular weight of 42.0 kDa and isoelectric point of 8.63 (Fig. 1a). BLASTX results revealed that Sp-inx2 was homologous to the innexin2 in *C. borealis*, *Homarus gammarus* and *Penaeus monodon* with identities of 56, 55 and 55%.

Sp-inx2 protein had five cysteine residues and there were two conserved cysteine residues in each extracellular loop. Compared to the published innexin protein sequences, Sp-inx2 protein also had four hydrophobic transmembrane domains as indicated by gray boxes in Fig. 1a.

3.2. Genomic organization of Sp-inx2

Based on Sp-inx2 cDNA sequences, the genomic DNA fragments were amplified and sequenced. The full-length Sp-inx2 genomic DNA was 3983 bp. Its genomic structure is shown in Fig. 1b. It consisted of five exons and four introns: the five exons were 363, 242, 222, 176 and 74 bp, and the four introns were 603, 601, 163 and 770 bp.

3.3. Multiple alignment of innexins

Multiple protein sequence alignment of Sp-inx2 with a selected group of fruit fly innexins is shown in Fig. 2.

The largest conservation among innexins is of the extracellular loops (two cysteines and a tryptophan), the YYQWV motif before the second transmembrane domain, an invariant proline and a tryptophan near the end of the second transmembrane domain, and a rather conserved tyrosine residue close to the beginning of the third transmembrane domain [19]. It was clear that the Sp-inx2 gene belonged to a conserved innexin gene family. Moreover, the proline residue in the second transmembrane domain was conserved in all known innexins and pannexins.

3.4. Phylogenetic analysis of Sp-inx2

The evolutionary relationship of Sp-inx2 with other innexins was predicted using a phylogenetic tree using the deduced amino

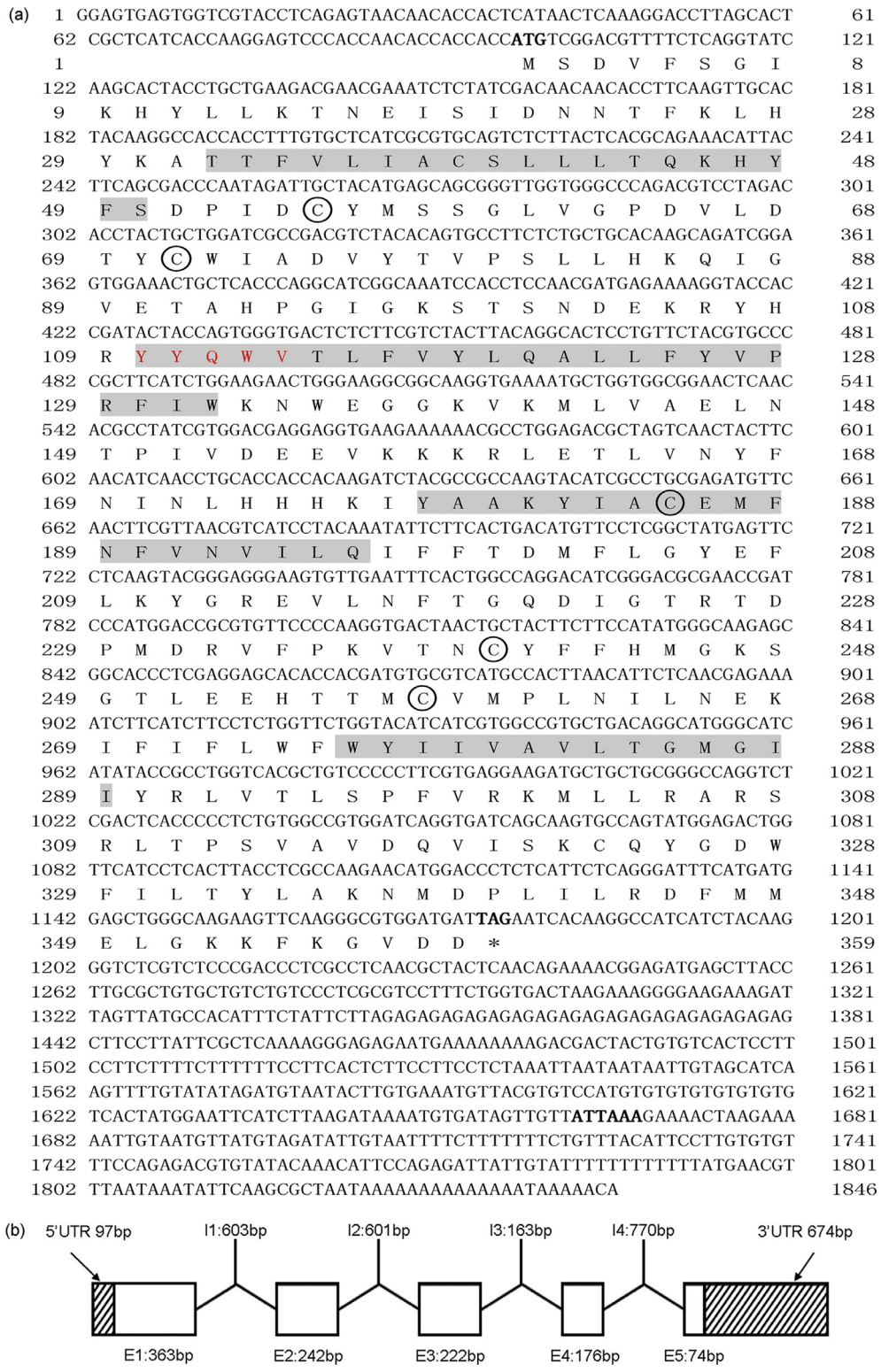

Fig. 1. (a) Sp-inx2 cDNA nucleotide sequence (above) and the deduced amino acid sequence of the ORF (below), and (b) the genomic DNA organization of the Sp-inx2 gene.

acid sequence (Fig. 3). BLAST analysis showed that Sp-inx2 had a high homology to innexin2 in other species. The deduced amino acid sequences of the innexin2 gene from 21 selected species are shown in Table 2. According to the NJ tree, innexin2 in insects were classified into the same cluster. Although *P. monodon*, *H. gammarus* and *S. paramamosain* all belong to the decapod order of crustaceans, the *P. monodon* and *H. gammarus* innexin2s were classified in the same cluster while the Sp-inx2 belonged to a new and independent clade. Although Sp-inx2 was weakly associated with the other innexin2 in arthropods, they were in a large branch. The tree also suggested that the nematode innexin2 had high sequence divergence from the arthropods. Because innexins and pannexins belong to the same gene superfamily, pannexin2 in the vertebrates was selected as an outgroup.

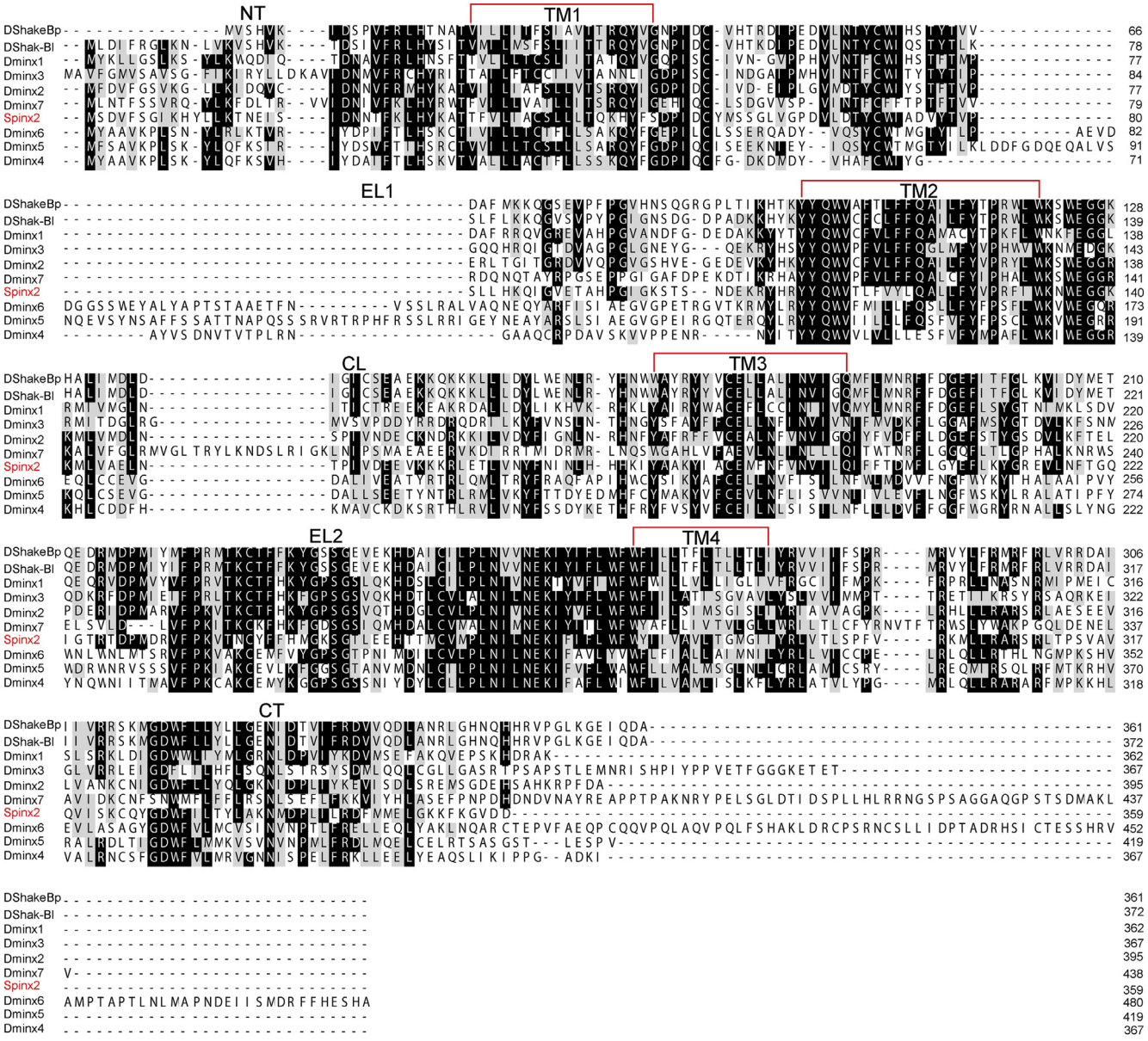

Fig. 2. Multiple alignment of the Sp-inx2 gene with the *Drosophila melanogaster* innexin gene family and the predicted transmembrane topology of Sp-inx2. The following innexins from *D. melanogaster* were included: Dm-inx1 (P27716), Dm-inx2 (AAD50379), Dm-inx3 (AAF50922), Dm-inx4 (AAF48923), Dm-inx5 (AAL25820), Dm-inx6 (AAL25821), Dm-inx7 (Q9V3W6), Dm-shakBl (AAB34769) and Dm-shakBp (NP523425).

3.5. Tissue distribution of Sp-inx2 mRNA and protein

qPCR was performed to study the tissue expression pattern of Sp-inx2 mRNA, with β-actin as the internal control. The results showed that Sp-inx2 mRNA transcripts were widely distributed in many tissues, and were most abundant in hemocytes, and then eyestalk and muscle tissue (Fig. 4a).

Western blotting was performed to examine Sp-inx2 protein levels in various tissues, using β-actin as the normalization control. The Sp-inx2 protein was detected in many tissues and was especially abundant in hemocytes (Fig. 4b). Immunofluorescence analysis also confirmed the Sp-inx2 expression in hemocytes (Fig. 4c).

3.6. Expression profiles of Sp-inx2 after bacterial exposure

To investigate whether the Sp-inx2 gene is involved in the *S. paramamosain* immune response, crabs were stimulated with LPSs, *V. alginolyticus*, or *V. parahaemolyticus*. Sp-inx2 mRNA levels in various tissues were measured at 3, 6, 12, 24, 48 or 96 h post infection using qPCR (Fig. 5).

The results showed that LPS stimulation increased Sp-inx2 mRNA expression in hemocytes in a time-dependent fashion. Sp-inx2 mRNA levels were significantly elevated at 3 and 6 h post-stimulation (3.57- and 2.08-fold higher than the control group, $p < 0.05$), and then returned to the baseline. Compared with the control group, there was no significant change from 12 to 96 h after LPS stimulation ($p > 0.05$). Sp-inx2 mRNA expression levels in the gill were not significantly different at any time post-stimulation except for a slight increase at 3 and 6 h ($p > 0.05$). Sp-inx2 mRNA expression was highest in the hepatopancreas 3 h post-stimulation (3.35-fold higher than the control group, $p < 0.05$).

With the challenge of *V. alginolyticus*, Sp-inx2 mRNA levels

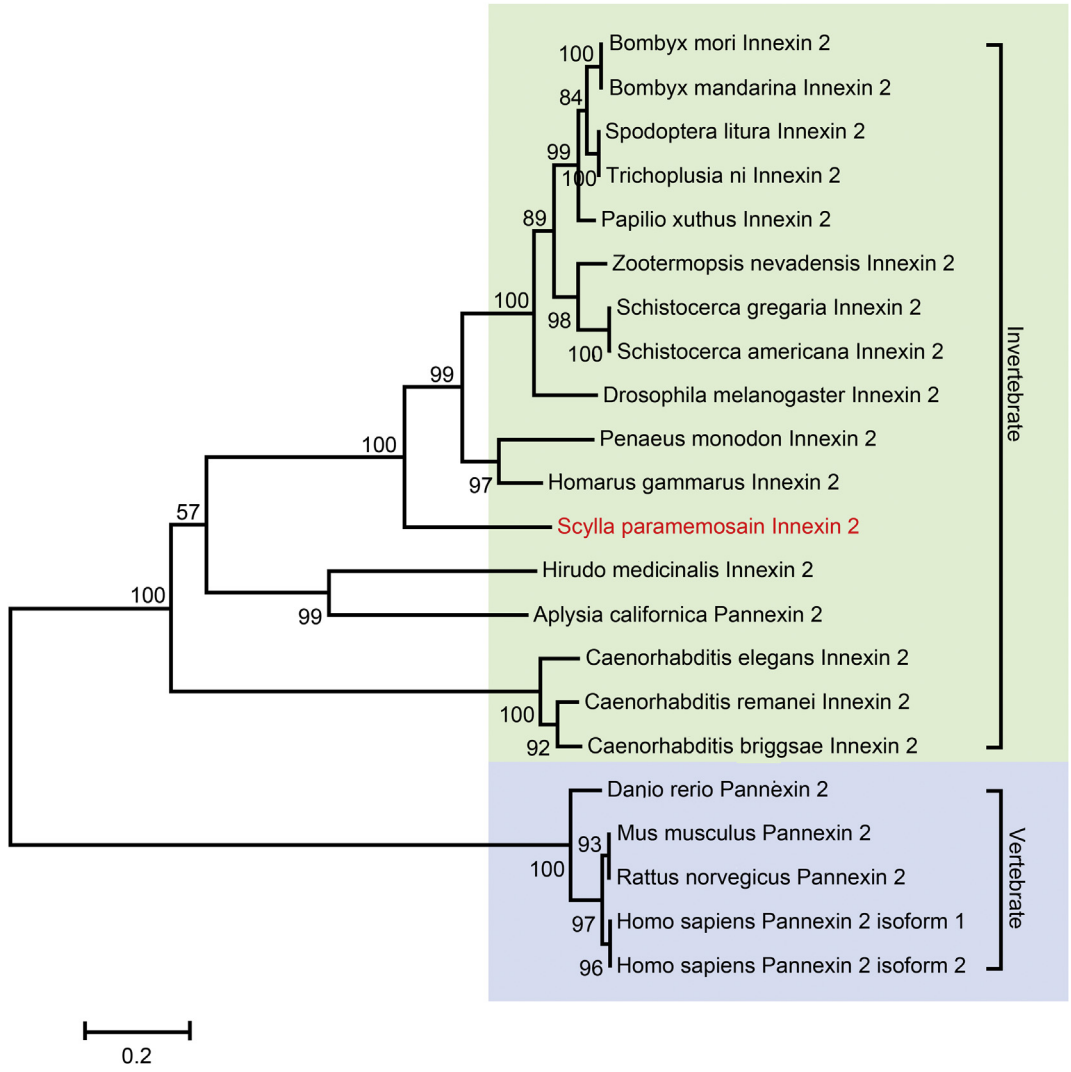

Fig. 3. Phylogenetic tree of innexin2 protein in various species. Numbers at branch nodes represent the confidence level of 1000 bootstrap replications. This NJ-tree was produced based on all members amino acid sequences. Accession numbers for these sequences are listed in Table 2.

Table 2
GenBank accession numbers of innexin 2 used in this study.

Species	Accession no.
Bmobyx mori	NP_001037203.1
Bmobyx mandarina	ABM88790.1
Spodoptera litura	AFY62975.1
Trichoplusia ni	AFY62977.1
Papilio xuthus	BAM19377.1
Zootermopsis nevadensis	KDR11527.1
Schistocerca gregaria	ACN41954.1
Schistocerca Americana	AAD29306.1
Drosophila melanogaster	AAF87943.1
Penaeus monodon	AGV55415.1
Homarus gammarus	CAJ58682.1
Scylla paramamosain	FJ774668.1
Hirudo medicinalis	CAD55802.1
Aplysia californica	NP_001191579.1
Caenorhabditis elegans	emb|CAB54206.2
Caenorhabditis remanei	EFO89680.1
Caenorhabditis briggsae	CAP35053.1
Danio rerio	NP_001243570.1
Mus musculus	EDL04385.1
Rattus norvegicus	CAD89523.1
Homo sapiens pax2 isoform 1	AAK91715.1
Homo sapiens pax2 isoform 2	NP_001153772.1

increased in all three tested tissues (hemocytes, gills and hepatopancreas). In the hemocytes, Sp-inx2 mRNA levels were 2.44- and 2.99-times that of the control ($p < 0.05$) at 3 and 6 h post challenge, and returned to baseline levels from 12 to 96 h ($p < 0.05$). Similarly, Sp-inx2 mRNA was significantly up-regulated in the gills at 3, 6 and 12 h post-challenge (3.85, 4.54 and 2.42-times higher than the control group, $p < 0.05$), and then decreased sharply from 24 to 96 h. In the hepatopancreas, Sp-inx2 mRNA expression was significantly up-regulated at 6 h post-challenge (2.13-times higher than the control group, $p < 0.05$), but was not significantly different from the control group at all other time points ($p > 0.05$) (Fig. 5).

With the challenge of *V. parahaemolyticus*, Sp-inx2 mRNA expression patterns were similar in the gills and hepatopancreas but different in the hemocytes. In all three tissues, Sp-inx2 mRNA expression reached its highest levels 3 h post-infection, especially in the gills (7.88–fold higher than the control group, $p < 0.05$) then gradually dropped back to baseline levels (Fig. 5).

Since hemocytes are the most important components of the crustacean immune system, we also examined the stimulatory effects of *E. coli* LPSs on Sp-inx2 expression in cultured hemocytes (Fig. 7a). The results showed that 200, but not 100 μg mL^{-1}, LPS-stimulation up-regulated Sp-inx2 mRNA transcription

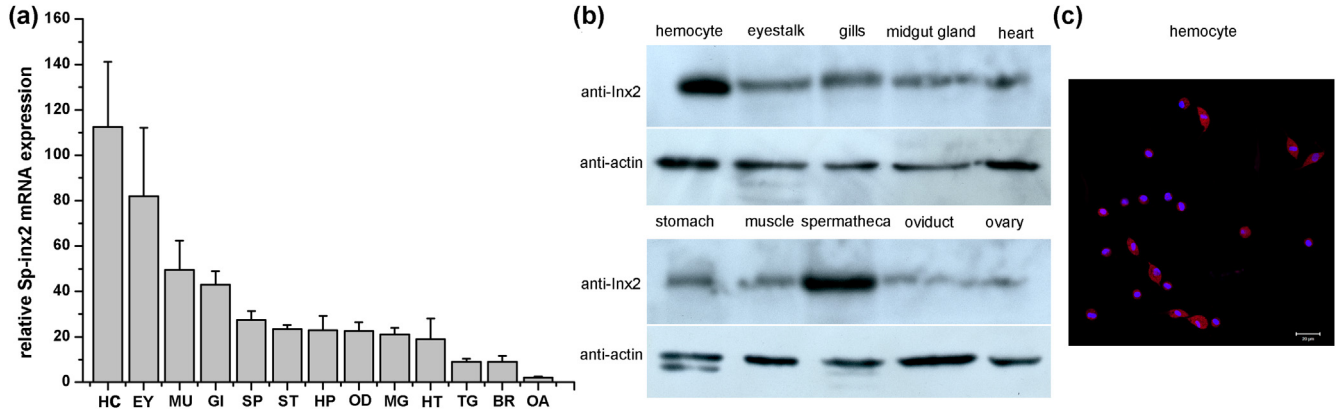

Fig. 4. (a) Sp-inx2 gene expression in different tissues, HC, hemocyte; EY, eyestalk; MU, muscle; GI, gills; SP, Spermatheca; ST, stomach; HP, hepatopancreas; OD, oviduct; MG, midgut gland; HT, heart; TG, thoracic ganglion mass; BR, brain; OA, ovary; (b) the Sp-inx2 protein levels in various tissues; and (c) the distribution of Sp-inx2 protein in hemocytes of *S. paramamosain*, Scale bar = 20 μm.

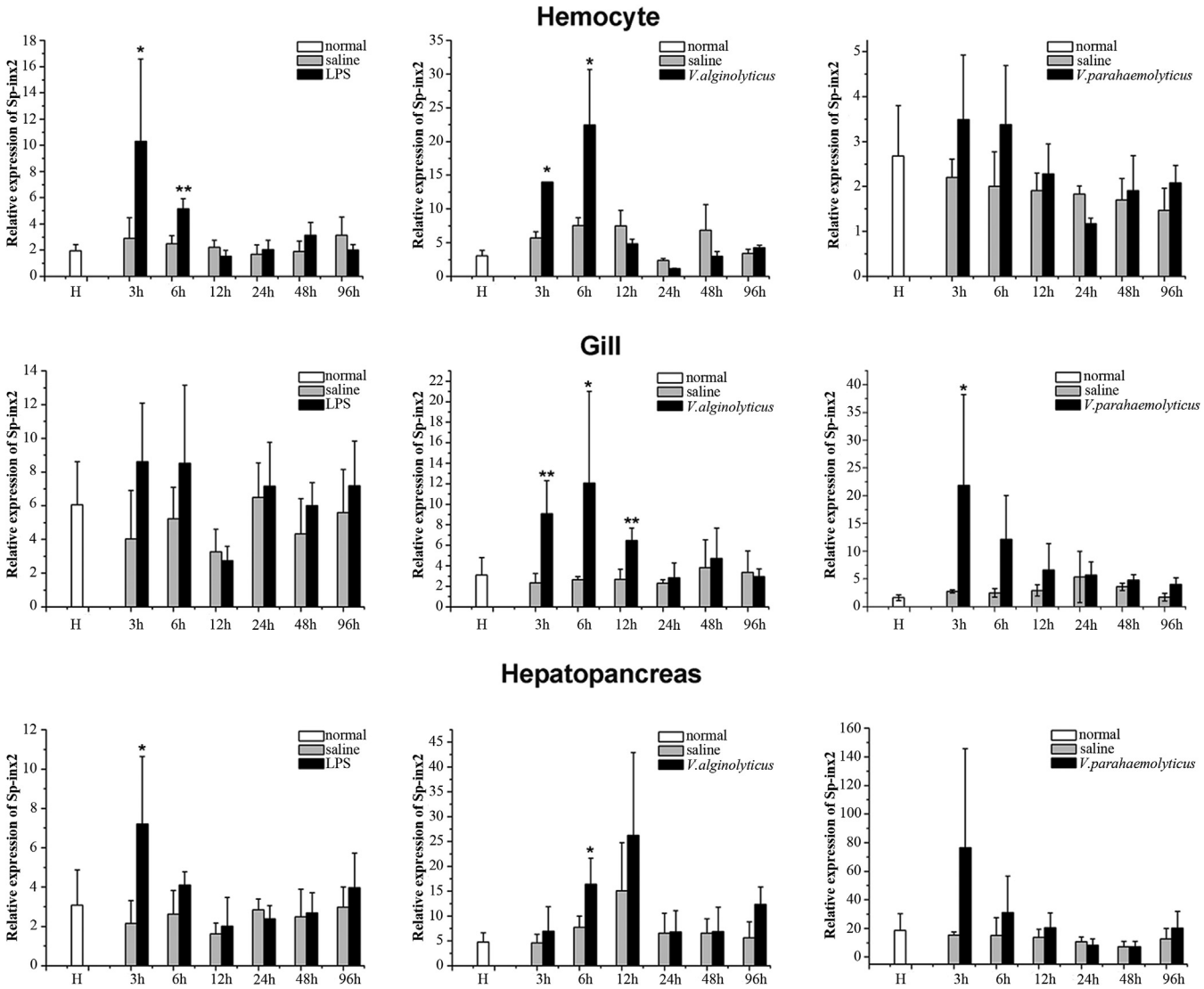

Fig. 5. Quantitative real-time PCR analysis of Sp-inx2 mRNA expression in various tissues of *S. paramamosain* injected with saline (control), or stimulated by LPSs, or infected by *V. alginolyticus* or *V. parahaemolyticus*. β-actin was used as an internal control. Box bars, the mean ± SD (N = 5). Asterisks indicate a significant difference with the control ($p < 0.05$ or $p < 0.01$).

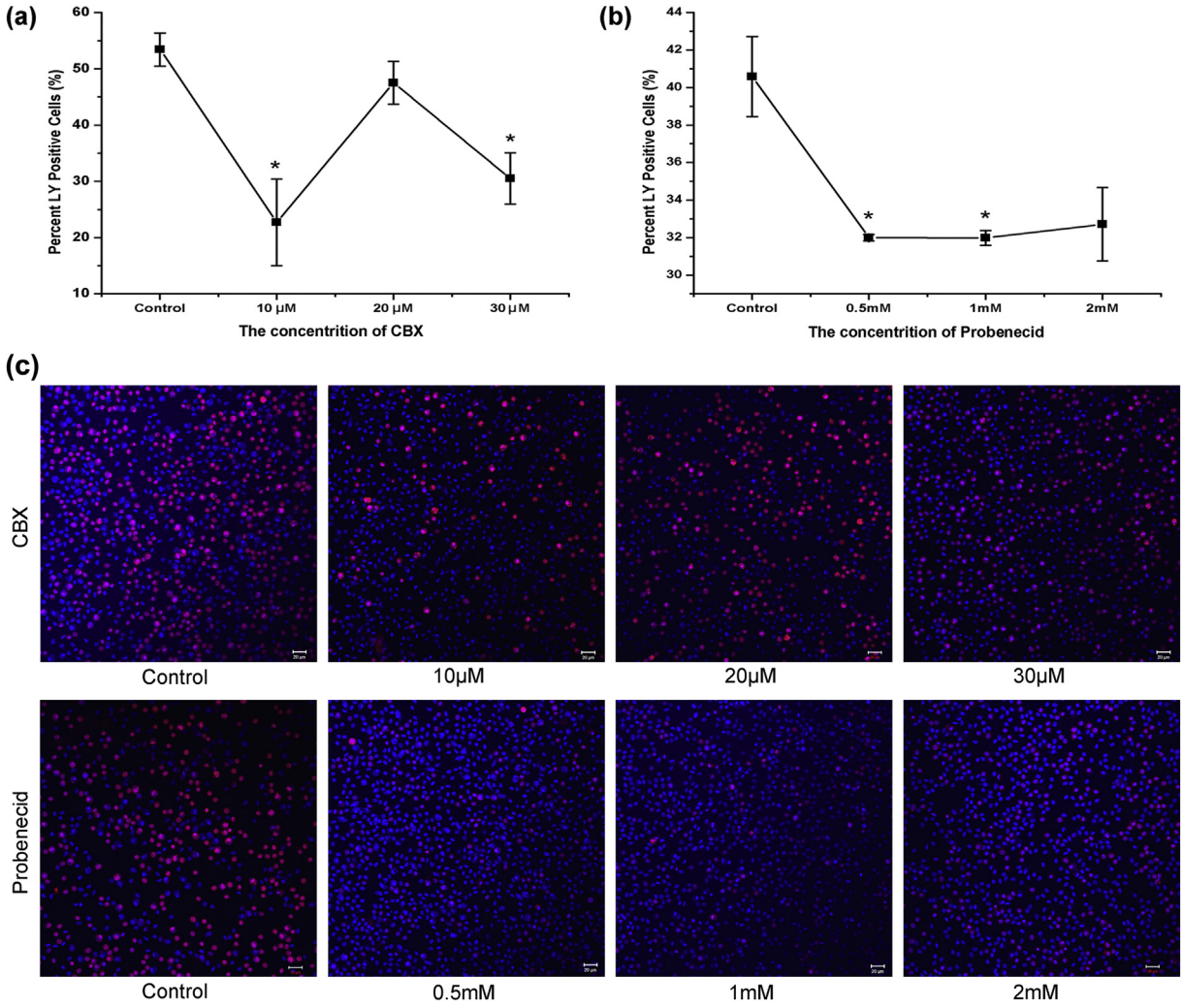

Fig. 6. Characterization of hemichannels in *Scylla paramamosain* hemocytes. The absorption rate of Lucifer yellow dye in hemocytes treated by (a) different concentrations of CBX (10, 20 or 30 μM), or (b) probenecid (0.5, 1 or 2 mM). Data are expressed as mean ± SD of three independent experiments. Asterisks indicate a significant difference with the control ($p < 0.05$); and (c) the inhibition effects of Lucifer yellow uptake at room temperature, as visualized in a laser scanning confocal microscope. Scale bar = 20 μm.

significantly ($p < 0.05$). Induction of the Sp-inx2 transcript lasted from 6 to 48 h with 200 μg mL^{-1} LPS stimulation, suggesting that the Sp-inx2 gene might be involved in hemocyte defense against LPS-stimulation.

Sp-inx2 protein levels in hemocytes stimulated with LPSs were also analyzed using Western blotting (Fig. 7b and c). Results showed that the change of Sp-inx2 protein level after LPS stimulation was not significant ($p > 0.05$). Even so, there was an increase in Sp-inx2 protein levels in hemocytes stimulated with 200 μg mL^{-1} LPS.

3.7. Identification of hemichannels in S. paramamosain hemocytes

In order to determine whether hemichannels exist in the crab hemocytes, we tested the ability of fluorochrome dye to pass through the cell membrane. The channels formed by innexin proteins allow the passage of both cationic and anionic dyes as well as the permeation of up to 1.5 kDa molecules [20]. The absorbance efficiency of LY (MW 457 Da) was established as a standard to evaluate channel activity. If the channels were functionally open, the LY dye would be rapidly transferred into the cell. If the channels were closed, the dye uptake rate would be reduced. Specific inhibitors can reduce the penetration ability of the dye. We found that CBX and probenecid both reduced the dye uptake rate in hemocytes (Fig. 6). CBX actively reduced dye uptake at concentrations of 10 or 30 μM, with rates of reduction of 57.51 and 42.92% ($p < 0.05$). However, 20 μM CBX did not reduce dye uptake for unknown reasons. The effect of probenecid on dye absorption was more consistent, especially at concentrations of 0.5 and 1 mM, with rates of reduction of 21.19 and 21.21% ($p < 0.05$).

3.8. Response of hemichannels after LPS stimulation

Following the observation in the study that Sp-inx2 mRNA and protein levels were up-regulated by LPS stimulation, we further investigated whether the innexin hemichannels were also affected. Results showed that the dye absorption rate of the crab hemocytes decreased 6 and 12 h after LPS stimulation (Fig. 7d and e). Compared to the control, there was a more than 60% rate reduction as measured with the LY/Hoechst diffusion ratio ($p < 0.01$). A minimal LY transfer rate was observed 6 h following 200 μg mL^{-1} LPS stimulation, with a reduction of 91.7% compared to the control group ($p < 0.01$). However, at 24 and 48 h post LPS stimulation, the values of LY transfer were similar to the control group ($p > 0.05$).

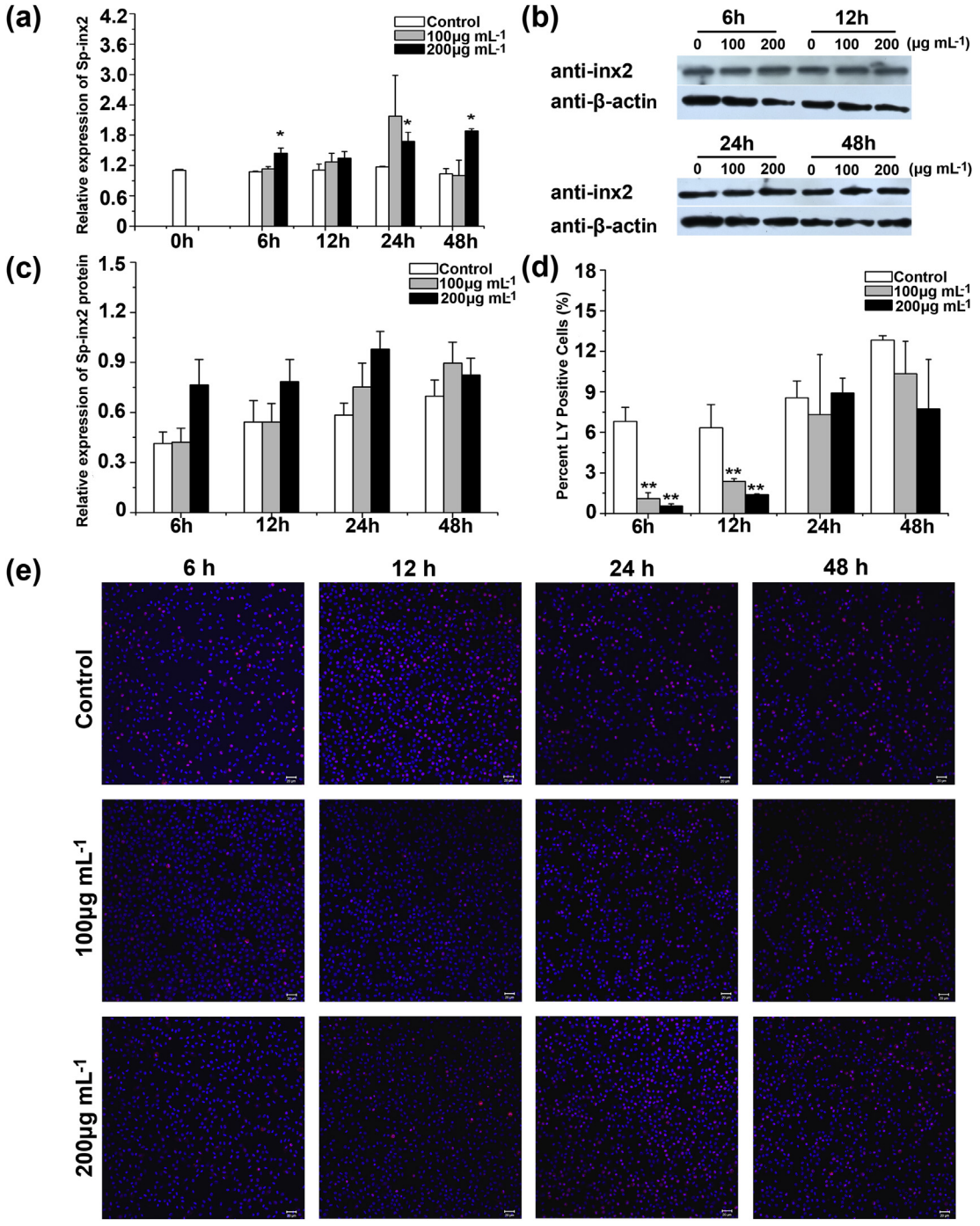

Fig. 7. Sp-inx2 mRNA level, protein level and hemichannels in hemocytes in response to LPS stimulation. Changes of Sp-inx2 (a) mRNA level, (b, c) protein expression when treated with two different concentrations (100 and 200 μg mL^{-1}) of LPSs. (d, e) LPS stimulation reduces hemocytes dye uptake. Images were captured using confocal microscopy. Scale bar = 20 μm. Data are expressed as mean ± SD of three independent experiments. Asterisks indicate a significant difference with the control ($p < 0.05$).

3.9. Response of innexins expressed in HeLa cells after LPS stimulation

Sp-inx2 proteins were ectopically expressed in HeLa cells (Fig. 8a) and mainly distributed in the cytoplasm and plasma membrane (Fig. 8b). Localization of Sp-inx2 in the plasma membrane suggested that it might form hemichannels on the cell surface. This possibility was tested using a red fluorescent dye uptake assay. We found that the dye uptake rate in HeLa cells ectopically expressing Sp-inx2 proteins was dramatically increased compared to the control ($p < 0.05$) (Fig. 8c and d), but, conversely, the dye uptake rate was significantly reduced with the addition of 50 μg mL^{-1} LPS ($p < 0.05$) (Fig. 8c and d). This result showed that Sp-inx2 formed hemichannels in HeLa cells, whereas LPSs effectively reduced the activity of the hemichannels, consistent with the observation in hemocytes.

3.10. Ectopic expression of Sp-inx2 promoted apoptosis in HeLa and EPC cells

When we observed that Sp-inx2 could be ectopically expressed in EPC (Fig. 9a) and HeLa cells (Fig. 9b), our study was extended to further understand whether the ectopic expression would alter the physiological status or cause some unusual functions in both cells.

Using a TUNEL assay and a confocal laser scanning microscope, we found that EPC cells ectopically expressing Sp-inx2 had higher levels of apoptosis than the control group, with a 1.91-fold increase in the cell apoptosis rate ($p < 0.05$) (Fig. 9a). The study further showed that EPC cells underwent a low level of apoptosis under normal culture conditions. Interestingly, more cell apoptosis was present in the HeLa cells which expressed Sp-inx2 proteins and the cell apoptosis rate increased by 30-fold compared with the control group ($p < 0.05$) (Fig. 9b). Furthermore, compared to the control group, the total number of HeLa cells in the experimental group was also reduced.

4. Discussion

Innexin proteins are commonly found in vertebrates and invertebrates but their functions remain largely unknown. In our study, a new innexin gene, Sp-inx2, was identified for the first time in the mud crab *S. paramamosain*, which is one of the most economically important mariculture crab species on the southeast coast of China. The deduced Sp-inx2 protein sequence showed a relatively high similarity with other invertebrate innexins (Fig. 2). The Sp-inx2 protein was predicted to have a structure similar to other innexins, with a typical four transmembrane topology, two ectodomains, one intracellular loop, and amino and carboxyl terminals in the cytosol (Fig. 2). In addition, there were two pairs of cysteine residues in the extracellular loop of the Sp-inx2 protein, unlike connexin in which there were three cysteine residues in each extracellular loop of the connexin proteins. The cysteine residues may form intra-innexin disulfide bonds for the correct polymer formation [21]. A proline residue in the second transmembrane domain is also present in all known innexins and pannexins. This conservation may be explained by the role of proline as an important component of a molecular hinge motif that acts as a conformational switch in response to voltage [22]. Pannexins have a complex gene structure, i.e., human pannexin2 has four coding exons and three introns, whereas mouse pannexin2 appears to have only three exons and two introns [23]. The Sp-inx2 identified in *S. paramamosain* had five exons and four introns (Fig. 1b). These findings reflected the diversity of innexin genomic DNA structures.

The results showed that Sp-inx2 mRNA and protein were widely expressed in various tissues of *S. paramamosain*, especially in the hemocytes (Fig. 4a and b). The wide tissue distribution of Sp-inx2 mRNA and protein suggested that it could be involved in multiplex biological functions in *S. paramamosain*. Our previous studies showed that there are three homologous innexins (Sp-inx1, Sp-inx2 and Sp-inx3) in *S. paramamosain*, but only Sp-inx2 mRNA and protein were dominantly expressed in the hemocytes (data not shown). Innexins are thought to form GJs or hemichannels in the cytomembrane of cells. While the positive labeling of cytoplasmic clouds or particles is presumed to indicate channel precursors [24], our results showed that the Sp-inx2 protein was also distributed in the cytoplasm of *S. paramamosain* hemocytes, and was not limited to the cytomembrane (Fig. 4c). We hypothesized that Sp-inx2 may oligomerize into distinct membrane pores in *S. paramamosain* hemocytes. This is why we not only characterized the Sp-inx2 gene and protein sequence as well as its functions, but also further investigated the physiological and functional roles of multimers formed by Sp-inx2.

Considering the high expression of Sp-inx2 in hemocytes and that Sp-inx2 was the up-regulated gene in the SSH cDNA library constructed from hemocytes in *S. paramamosain* in response to LPSs, we speculated that Sp-inx2 may play an important role in the innate immune defense. Hemocytes, gills and hepatopancreas are important organs involved in crustacean immunity and play a key role in the immune response. Hemocytes are essential for many processes, including transport and digestion of nutrients and immune defense [25]. The gills represent the main interface between aquatic organisms and the external environment, so it is the first line of defense against bacterial infection [26]. The hepatopancreas is very susceptible to the infection of various pathogens, and many diseases can be diagnosed based on its pathological changes and abnormalities in its physiological state [27]. Sp-inx2 mRNA transcripts were significantly up-regulated in the early period after stimulation with LPSs, *V. alginolyticus* or *V. parahaemolyticus* (Fig. 5). Both *V. alginolyticus* and *V. parahaemolyticus* are gram-negative bacteria which are responsible for approximately one-third of aquaculture disease cases [28]. LPSs are a major component of the outer membrane of the gram-negative bacteria and can initiate potent innate immune responses that prime the immune system against further infection [29]. Upon LPS stimulation and *V. alginolyticus* infection, Sp-inx2 transcripts were significantly up-regulated in hemocytes at 3 and 6 h, respectively. Sp-inx2 expression was up-regulated in gills following *V. alginolyticus* infection at 3, 6 and 12 h, and *V. parahaemolyticus* infection at 3 h. Up-regulation of Sp-inx2 was also observed in the hepatopancreas 6 h post-*V. alginolyticus* injection and 3 h post LPS stimulation. These results suggested that Sp-inx2 was involved in the early immune defense against gram-negative bacteria. Previous studies report that pannexin1 plays an important role in the release of extracellular ATP, an essential ligand for the activation of purinergic signaling in *Paralichthys olivaceus* innate immunity [30]. The presence of LPSs could increase the expression of pannexin1 and inflammasome components in hepatocytes, which primes them for IL-1β release and ATP-dependent apoptosis [31–34]. Thus, Sp-inx2 transcript up-regulation may be a common response of *S. paramamosain* primary immune system when exposed to gram-negative bacteria or LPSs.

Early studies on the pharmacological properties of hemichannels rely on the use of CBX, probenecid, flufenamic acid, glycyrrhetinic acid (GA) derivatives (18 α-GA), Brilliant Blue G etc [35]. These drugs inhibit currents mediated by the hemichannels [36]. To understand the physiological properties of innexons formed by innexin in *S. paramamosain* hemocytes, effective and relatively specific drugs that inhibit hemichannel activity are desirable. CBX is a synthetic derivative of GA that has been used to block connexin-based channels for nearly 30 years [37], and it can also block the currents in pannexin and innexin formed channels [31,36]. Probenecid was also an effective inhibitor for pannexin channels. In our study, both CBX and probenecid reduced crab hemocyte dye uptake (Fig. 6). These results demonstrated that hemichannels composed of innexins indeed exist in *S. paramamosain* hemocytes. Since *S. paramamosain* hemocytes consist of a mixed population of hyaline cells, semigranular cells and granular cells, whether each type of hemocyte has hemichannels composed of innexin proteins is left to be further investigated.

LPSs can reduce [38], increase [39], or have no effect on connexin gene expression [40], and modify connexin protein post-translationally [38,41]. Moreover, the dye uptake capability of the hemichannel is down-regulated in High Five cells in the presence of LPSs [18]. In our study, the dye uptake rate in hemocytes was significantly reduced by LPS stimulation at 6 and 12 h, which suggested that LPSs might reduce hemichannel activity, weaken the communication between cells and reduce the transport of substances inside and outside the cells (Fig. 7d and e). However, the Sp-inx2 mRNA and protein level increased from 6 to 48 h after LPS challenge, which inferred that the up-regulation of Sp-inx2 may be a compensation effect for the decrease of hemichannel activity (Fig. 7a, b and c). Therefore, the down-regulation of hemichannel activity and up-regulation of Sp-inx2 in hemocytes challenged with LPSs may reflect a host defense response to LPSs. The dye uptake

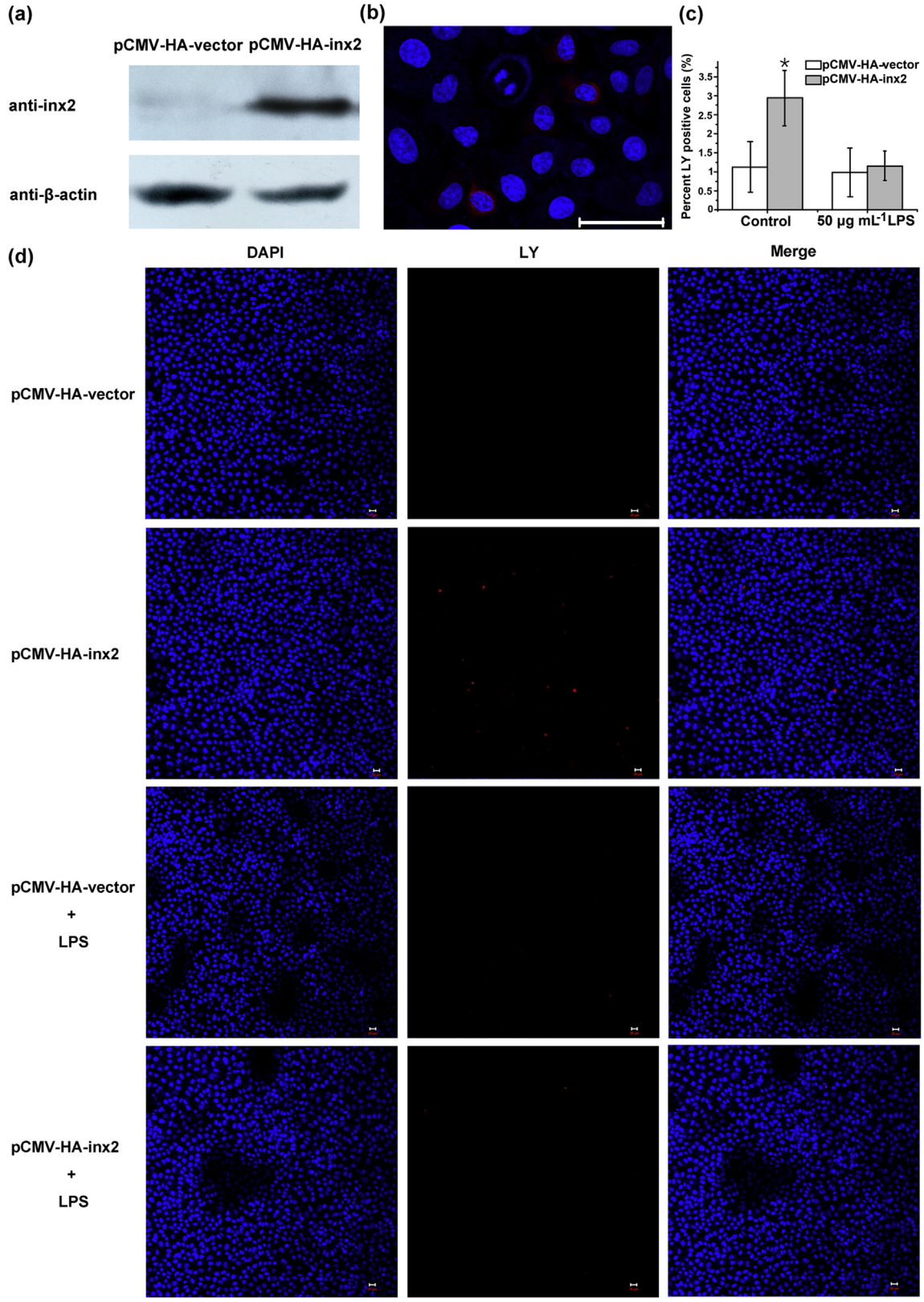

Fig. 8. (a) Western blotting of Sp-inx2 protein in HeLa cells transfected by pCMV-HA-Sp-inx2 or pCMV-HA-vector. (b) Immunofluorescence images of HeLa cells ectopically expressing Sp-inx2 protein, Scale bar = 50 μm (c, d) Dye uptake of HeLa cells transfected with pCMV-HA-Sp-inx2 was inhibited by LPS stimulation. Images were captured using confocal microscopy. Scale bar = 20 μm. Data are expressed as mean ± SD of three independent experiments. Asterisks indicate a significant difference with the control ($p < 0.05$).

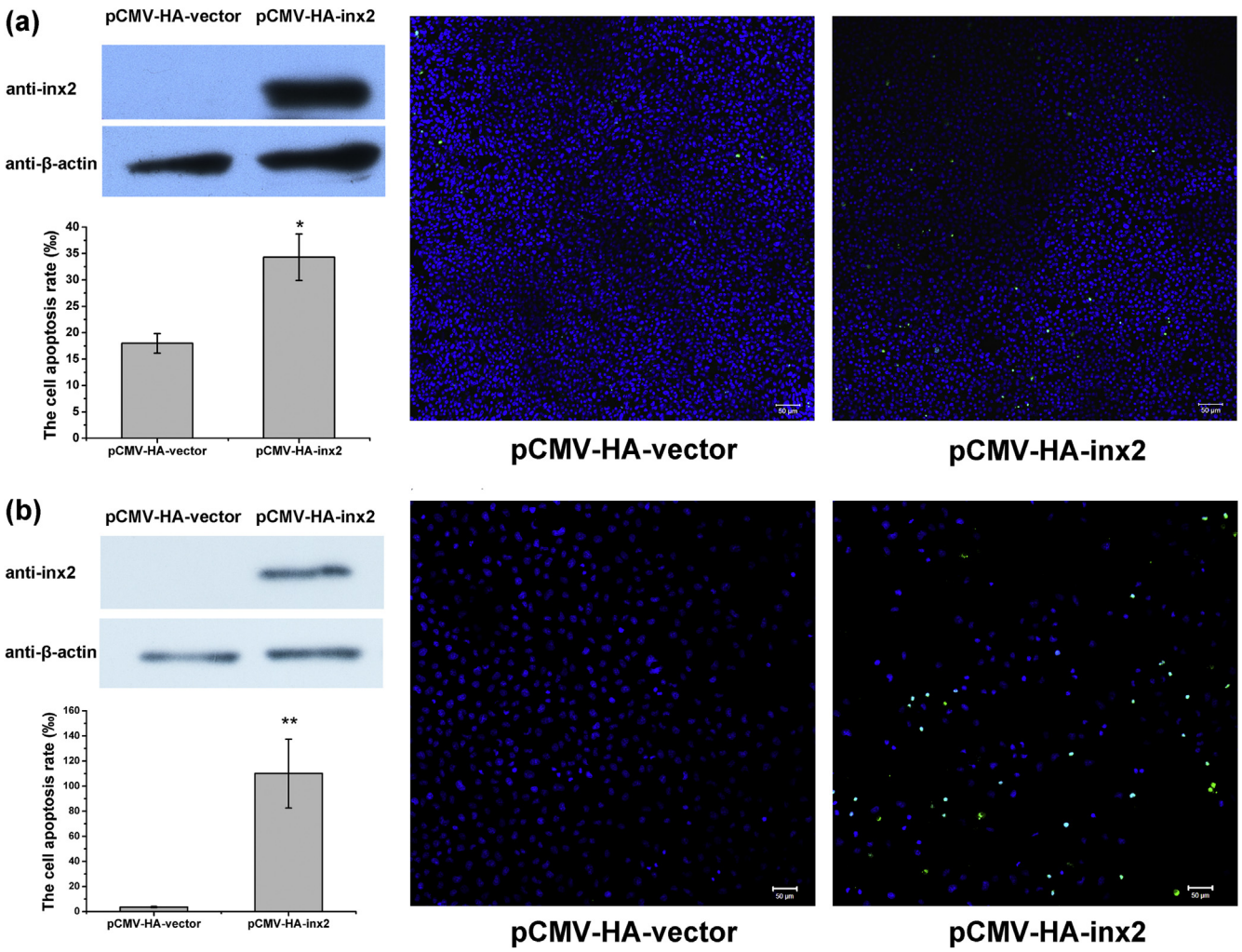

Fig. 9. Ectopic expression of Sp-inx2 promotes apoptosis in (a) EPC cells and (b) HeLa cells. The images of Western blotting represent the expression of Sp-inx2 protein or the control. The histogram represents the change of apoptosis rate. One or two asterisks indicate significant differences with the control ($p < 0.05$ or 0.01), respectively. The images were captured using confocal microscopy indicating apoptosis. Assays were repeated at least three times.

activity down-regulation of hemichannels in hemocytes might be due to closure of the channel but not the degradation of the innexin protein. The reduction in hemichannel activity following LPS stimulation could be explained as follows: hemichannels may act as pathogenic pores that probably cause cell death, the subsequent closure of hemichannels could be explained as having a cell-protective purpose as described previously [42]. Other reports also show that the activity of hemichannels is inhibited by kinases, such as PKC or Src [43,44]. The underlying mechanism may involve kinase activation by LPSs suppressing hemichannels [45]. In addition, some hemichannels can mediate paracrine signaling by providing a flux pathway for ions such as Ca^{2+}, ATP, glutamate and possibly other compounds [12], among which ATP is an energy metabolism molecular which can travel across the hemichannels [46]. Although it was observed that the passage of fluorescent dye through hemichannels was obviously inhibited following LPS challenge, there was no direct evidence that ATP release, hemocyte hemichannel activity and LPS stimulation interconnect.

The Sp-inx2 protein was successfully ectopically expressed in HeLa cells (Fig. 8a and b) and the dye absorbance rate were significantly increased 72 h after the transfection of the pCMV-HA-Sp-inx2 plasmid (Fig. 8c), suggesting that this cell line could be used as a model system to study the intrinsic properties of innexins. The formation of active polymers laid the foundation for future study of the hemichannel functions. Similar findings are observed in pannexin1 protein overexpressed C6 glioma cells [47] and HeLa cells [48]. It is well known that hemichannels do not function as free-floating entities in the plasma membrane but interact with specific cytoplasmic proteins that link them to the cytoskeleton and to intracellular signal pathways [12]. Therefore, the interaction of innexin, cytoplasmic proteins and related signal transduction pathways should also be elucidated in future.

In this study, the dye uptake of HeLa cells expressing Sp-inx2 proteins was effectively inhibited by LPSs, indicating that Sp-inx2 protein may form hemichannels in HeLa cells and that the hemichannel activity could be inhibited by LPSs (Fig. 8c and d). Since similar results were observed in hemocytes and HeLa cells, this response might be a positive defense mechanism for these cells, which could also cause disorders such as homeostatic imbalances [38]. Previous studies point out that LPSs potentiate ATP release via hemichannels in C6-connexin43 cells, and also inhibit ATP release in HeLa-connexin43 cells. This difference may be cell-type dependent [45]. However, a number of basic channel properties and stimulus-based regulatory mechanisms are still largely unclear.

The hemichannels of connexin43 in vertebrate are associated with apoptosis [49]. When the activities of hemichannels decline,

the content of apoptosis-associated proteins caspase and BID decrease and the content of extracellular ATP declines as well [49]. The cell death process is slowed by silencing the gene expression of connexin32 or inhibiting its channel activities [50]. Ectopic expression of innexin2 and innexin3 promotes apoptosis in Sf9 cells and over-expression of innexin2 and innexin3 contributes to apoptosis in Spli221 cells [15]. Formation of hemichannels also facilitates the apoptotic-to-necrotic transition [51]. Converting the intracellular residue C346 or the transmembrane residue C40 of pannexin1 to serine results in a constitutively open channel that rapidly degrades plasma membrane potentials, leading finally to cell death [12,21,52,53]. In our study, ectopic-expression of Sp-inx2 protein promoted apoptosis in both EPC and HeLa cells (Fig. 9). The explanation of this phenomenon may be that expression of Sp-inx2 inhibited HeLa cell proliferation by inducing apoptosis. This result showed that Sp-inx2 protein was involved in regulating cell apoptosis, which was consistent with the results of previous studies.

The fact that ectopically expressed Sp-inx2 promotes apoptosis has several possible explanations. First, the active hemichannel might be involved in some paracrine signaling pathways related to apoptosis. Hemichannel activation can inhibit PI3K/AKT signaling [15], which is one of the most important pathways in the regulation of cell survival. Secondly, hemichannel activation may lead to increased $[Ca^{2+}]_i$ release from the endoplasmic reticulum, which causes mitochondrial outer membrane permeabilization (MOMP). As is known, MOMP is an apoptosis-inducing factor, which triggers a cascade of events including the release of mitochondrial cytochrome C, activation of the caspases cascade and ultimately apoptosis [54]. During the process, caspase-3 may reversibly cleave the carboxyl terminal of innexin, which probably activates this channel, causing more cell death [16]. Thus, excessive signaling through this pathway could enhance the induction of apoptosis. Thirdly, we found Sp-inx2 not only in the plasma membrane but also abundantly associated with the cytoplasm, possibly in the organelle membranes as well. A previous study shows that connexin43 localizes to the Golgi apparatus and mitochondria [49]. Thus, if the Sp-inx2 hemichannels localize in the mitochondria of HeLa and EPC cells, this would directly play a role in the permeabilization of this organelle and subsequently cell apoptosis. As reported, those connexins that do not form channels can also participate in apoptotic pathways by interacting with factors related to apoptosis [51]. Therefore, there would be the possibility that the ectopically expressed Sp-inx2 protein itself or the hemichannels composed of Sp-inx2 proteins could promote cell apoptosis.

Connexins and pannexins negatively regulate the tumor cell growth; and evidence suggests that the shape of C6 glioma cell transfected pannexin1 gene changes from the normal spindle shape to a flat shape. Stable expression of pannexin1 in C6 cells significantly reduces cell proliferation in monolayers, cell motility, anchorage-independent growth, and in vivo tumor growth in athymic nude mice [47]. Other studies also show that, after the connexin43 cDNA is transfected into C6 glioma cells, cell proliferation is significantly reduced; cell volume becomes bigger; shape flattens; and malignant phenotype characteristics become blurry [55]. Once the human tumor cells (SKHepl) are transfected connexin32 cDNA, the cells can turn from the “zero gap junction intercellular communication state” to “normalization”, whereas the cell growth is greatly inhibited [56]. In our study, we noted that the HeLa and EPC cells in which the Sp-inx2 protein was ectopically expressed could increase the cell apoptosis. This result suggested that Sp-inx2 protein may be involved in antitumor activity.

The present study first reported a new hemichannel-associated transmembrane protein named as Sp-inx2 identified in *S. paramamosain*. It was found that Sp-inx2 was likely to be involved in the function associated with immune response and apoptosis. Sp-inx2 or Sp-inx2-formed hemichannels probably participate in cell regulation through different signaling pathways. The evidence collected in our study suggested that Sp-inx2 would play key roles in immunity and cell apoptosis in the marine mud crabs.

Acknowledgments

This work was supported by grants (U1205123, 41176116) from the National Natural Science Foundation of China (NSFC), and by a grant (2012N0019) from the Fujian Science and Technology Department. Professor John Hodgkiss of The University of Hong Kong is thanked for his assistance with English.

References

[1] Y.V. Panchin, Evolution of gap junction proteins–the pannexin alternative, J. Exp. Biol. 208 (2005) 1415–1419.
[2] G. Söhl, S. Maxeiner, K. Willecke, Expression and functions of neuronal gap junctions, Nat. Rev. Neurosci. 6 (2005) 191–200.
[3] V.M. Unger, N.M. Kumar, N.B. Gilula, M. Yeager, Projection structure of a gap junction membrane channel at 7 A resolution, Nat. Struct. Biol. 4 (1997) 39–43.
[4] R. Bauer, B. Löer, K. Ostrowski, J. Martini, A. Weimbs, H. Lechner, et al., Intercellular communication: the Drosophila innexin multiprotein family of gap junction proteins, Chem. Biol. 12 (2005) 515–526.
[5] Z.F. Altun, B. Chen, Z.W. Wang, D.H. Hall, High resolution map of *Caenorhabditis elegans* gap junction proteins, Dev. Dyn. 238 (2009) 1936–1950.
[6] B. Kandarian, J. Sethi, A. Wu, M. Baker, N. Yazdani, E. Kym, et al., The medicinal leech genome encodes 21 innexin genes: different combinations are expressed by identified central neurons, Dev. Genes Evol. 222 (2012) 29–44.
[7] S. Shruti, D.J. Schulz, K.M. Lett, E. Marder, Electrical coupling and innexin expression in the stomatogastric ganglion of the crab *Cancer borealis*, J. Neurophysiol. 112 (11) (2014) 2946–2958.
[8] K.R. Norman, A.V. Maricq, Innexin function: minding the gap junction, Curr. Biol. 17 (2007) R812–R814.
[9] M. Herrera, M.J. Bastiani, Developmental expression and molecular characterization of two gap junction channel proteins expressed during embryogenesis in the grasshopper *Schistocerca americana*, Dev. Genet. 24 (1999) 137–150.
[10] R. Bauer, C. Lehmann, B. Fuss, F. Eckardt, M. Hoch, The Drosophila gap junction channel gene innexin2 controls foregut development in response to Wingless signalling, J. Cell Sci. 115 (2002) 1859–1867.
[11] T. Ayukawa, K. Matsumoto, H.O. Ishikawa, A. Ishio, T. Yamakawa, N. Aoyama, et al., Rescue of Notch signaling in cells incapable of GDP-L-fucose synthesis by gap junction transfer of GDP-L-fucose in Drosophila, Proc. Natl. Acad. Sci. 109 (2012) 15318–15323.
[12] J.C. Hervé, M. Derangeon, Gap-junction-mediated cell-to-cell communication, Cell Tissue Res. 352 (2013) 21–31.
[13] S.E. Adamson, N. Leitinger, The role of pannexin1 in the induction and resolution of inflammation, FEBS Lett. 588 (2014) 1416–1422.
[14] S. Locovei, J.J. Wang, G. Dahl, Activation of pannexin1 channels by ATP through P2Y receptors and by cytoplasmic calcium, FEBS Lett. 580 (2006) 239–244.
[15] T. Liu, M. Li, Y. Zhang, Z. Pang, W. Xiao, Y. Yang, et al., A role for Innexin2 and Innexin3 proteins from *Spodoptera litura* in apoptosis, PloS One 8 (2013) e70456.
[16] F.B. Chekeni, M.R. Elliott, J.K. Sandilos, S.F. Walk, J.M. Kinchen, E.R. Lazarowski, et al., Pannexin1 channels mediate ‘find-me’ signal release and membrane permeability during apoptosis, Nature 467 (2010) 863–867.
[17] F.Y. Chen, H.P. Liu, J. Bo, H.L. Ren, K.J. Wang, Identification of genes differentially expressed in hemocytes of *Scylla paramamosain* in response to lipopolysaccharide, Fish Shellfish Immunol. 28 (2010) 167–177.
[18] K. Luo, M.W. Turnbull, Characterization of nonjunctional hemichannels in caterpillar cells, J. Insect Sci. 11 (2011) 6.
[19] F. Abascal, R. Zardoya, Evolutionary analyses of gap junction protein families, Biochim. Biophys. Acta (BBA)-Biomembr. 1828 (2013) 4–14.
[20] J. Wang, M. Ma, S. Locovei, R.W. Keane, G. Dahl, Modulation of membrane channel currents by gap junction protein mimetic peptides: size matters, Am. J. Physiol. Cell Physiol. 293 (2007) C1112–C1119.
[21] S. Bunse, M. Schmidt, N. Prochnow, G. Zoidl, R. Dermietzel, Intracellular cysteine 346 is essentially involved in regulating Panx1 channel activity, J. Biol. Chem. 285 (2010) 38444–38452.
[22] M.S. Sansom, H. Weinstein, Hinges, swivels and switches: the role of prolines in signalling via transmembrane α-helices, Trends Pharmacol. Sci. 21 (2000) 445–451.
[23] S. Penuela, D.W. Laird, The cellular life of pannexins, Wiley Interdiscip. Rev.

Membr. Transp. Signal. 1 (2012) 621–632.
[24] J. Bohrmann, J. Zimmermann, Gap junctions in the ovary of *Drosophila melanogaster*: localization of innexins1, 2, 3 and 4 and evidence for intercellular communication via innexin2 containing channels, BMC Dev. Biol. 8 (2008) 111.
[25] A. Tame, T. Yoshida, K. Ohishi, T. Maruyama, Phagocytic activities of hemocytes from the deep-sea symbiotic mussels *Bathymodiolus japonicus, B. platifrons*, and *B. septemdierum*, Fish Shellfish Immunol. 45 (2015) 146–156.
[26] A. Lichtenfels, G. Lorenzi-Filho, E. Guimaraes, M. Macchione, P. Saldiva, Effects of water pollution on the gill apparatus of fish, J. Comp. Pathol. 115 (1996) 47–60.
[27] J. Du, H. Zhu, P. Liu, J. Chen, Y. Xiu, W. Yao, et al., Immune responses and gene expression in hepatopancreas from *Macrobrachium rosenbergii* challenged by a novel pathogen spiroplasma MR-1008, Fish Shellfish Immunol. 34 (2013) 315–323.
[28] L. Tang, Y. Liang, Y. Jiang, S. Liu, F. Zhang, X. He, et al., Identification and expression analysis on bactericidal permeability-increasing protein/lipopolysaccharide-binding protein of blunt snout bream, *Megalobrama amblycephala*, Fish Shellfish Immunol. 45 (2015) 630–640.
[29] B.S. Park, J.-O. Lee, Recognition of lipopolysaccharide pattern by TLR4 complexes, Exp. Mol. Med. 45 (2013) e66.
[30] S. Li, X. Li, X. Chen, X. Geng, J. Sun, ATP release channel Pannexin1 is a novel immune response gene in Japanese flounder *Paralichthys olivaceus*, Fish Shellfish Immunol. 40 (2014) 164–173.
[31] S.R. Bond, C.C. Naus, The pannexins: past and present, Front. Physiol. 5 (58) (2014) 1–24.
[32] T. Csak, M. Ganz, J. Pespisa, K. Kodys, A. Dolganiuc, G. Szabo, Fatty acid and endotoxin activate inflammasomes in mouse hepatocytes that release danger signals to stimulate immune cells, Hepatology 54 (2011) 133–144.
[33] M. Ganz, T. Csak, B. Nath, G. Szabo, Lipopolysaccharide induces and activates the Nalp3 inflammasome in the liver, World J. gastroenterol. WJG 17 (2011) 4772.
[34] F. Xiao, S.L. Waldrop, A-k. Khimji, G. Kilic, Pannexin1 contributes to pathophysiological ATP release in lipoapoptosis induced by saturated free fatty acids in liver cells, Am. J. Physiol. Cell Physiol. 303 (2012) C1034–C1044.
[35] A.W. Lohman, B.E. Isakson, Differentiating connexin hemichannels and pannexin channels in cellular ATP release, FEBS Lett. 588 (2014) 1379–1388.
[36] W. Silverman, S. Locovei, G. Dahl, Probenecid, a gout remedy, inhibits pannexin 1 channels, Am. J. Physiol. Cell Physiol. 295 (2008) C761–C767.
[37] J.S. Davidson, I.M. Baumgarten, E.H. Harley, Reversible inhibition of intercellular junctional communication by glycyrrhetinic acid, Biochem. Biophys. Res. Commun. 134 (1986) 29–36.
[38] A. De Maio, C. Gingalewski, N.G. Theodorakis, M.G. Clemens, Interruption of hepatic gap junctional communication in the rat during inflammation induced by bacterial lipopolysaccharide, Shock 14 (2000) 53–59.
[39] A. Temme, T. Ott, T. Haberberger, O. Traub, K. Willecke, Acute-phase response and circadian expression of connexin26 are not altered in connexin32-deficient mouse liver, Cell Tissue Res. 300 (2000) 111–117.
[40] E. Oviedo-orta, T. Hoy, W.H. Evans, Intercellular communication in the immune system: differential expression of connexin40 and 43, and perturbation of gap junction channel functions in peripheral blood and tonsil human lymphocyte subpopulations, Immunology 99 (2000) 578–590.
[41] C. Gingalewski, K. Wang, M.G. Clemens, A. De Maio, Posttranscriptional regulation of connexin 32 expression in liver during acute inflammation, J. Cell. Physiol. 166 (1996) 461–467.
[42] W. Evans, E. De Vuyst, L. Leybaert, The gap junction cellular internet: connexin hemichannels enter the signalling limelight, Biochem. J. 397 (2006) 1–14.
[43] H. Li, T.F. Liu, A. Lazrak, C. Peracchia, G.S. Goldberg, P.D. Lampe, et al., Properties and regulation of gap junctional hemichannels in the plasma membranes of cultured cells, J. Cell Biol. 134 (1996) 1019–1030.
[44] X. Bao, G.A. Altenberg, L. Reuss, Mechanism of regulation of the gap junction protein connexin43 by protein kinase C-mediated phosphorylation, Am. J. Physiol. Cell Physiol. 286 (2004) C647–C654.
[45] E. De Vuyst, E. Decrock, M. De Bock, H. Yamasaki, C.C. Naus, W.H. Evans, et al., Connexin hemichannels and gap junction channels are differentially influenced by lipopolysaccharide and basic fibroblast growth factor, Mol. Biol. Cell. 18 (2007) 34–46.
[46] S.E. Samuels, J.B. Lipitz, G. Dahl, K.J. Muller, Neuroglial ATP release through innexin channels controls microglial cell movement to a nerve injury, J. General Physiol. 136 (2010) 425–442.
[47] C.P. Lai, J.F. Bechberger, R.J. Thompson, B.A. MacVicar, R. Bruzzone, C.C. Naus, Tumor-suppressive effects of pannexin1 in C6 glioma cells, Cancer Res. 67 (2007) 1545–1554.
[48] S.R. Bond, N. Wang, L. Leybaert, C.C. Naus, Pannexin1 ohnologs in the teleost lineage, J. Membr. Biol. 245 (2012) 483–493.
[49] M. Vinken, E. Decrock, T. Vanhaecke, L. Leybaert, V. Rogiers, Connexin43 signaling contributes to spontaneous apoptosis in cultures of primary hepatocytes, Toxicol. Sci. 125 (2012) 175–186.
[50] E. Decrock, M. Vinken, E. De Vuyst, D. Krysko, K. D'Herde, T. Vanhaecke, et al., Connexin-related signaling in cell death: to live or let die? Cell Death Differ. 16 (2009) 524–536.
[51] M. Vinken, E. Decrock, E. De Vuyst, M. De Bock, R.E. Vandenbroucke, B.G. De Geest, et al., Connexin32 hemichannels contribute to the apoptotic-to-necrotic transition during Fas-mediated hepatocyte cell death, Cell. Mol. Life Sci. 67 (2010) 907–918.
[52] S. Bunse, M. Schmidt, S. Hoffmann, K. Engelhardt, G. Zoidl, R. Dermietzel, Single cysteines in the extracellular and transmembrane regions modulate pannexin1 channel function, J. Membr. Biol. 244 (2011) 21–33.
[53] J. Wang, G. Dahl, SCAM analysis of Panx1 suggests a peculiar pore structure, J. General Physiol. 136 (2010) 515–527.
[54] J. Davidson, C. Green, L. Bennet, A. Gunn, Battle of the hemichannels–Connexins and Pannexins in ischemic brain injury, Int. J. Dev. Neurosci. 45 (2015) 66–74.
[55] D. Zhu, S. Caveney, G. Kidder, C. Naus, Transfection of C6 glioma cells with connexin43 cDNA: analysis of expression, intercellular coupling, and cell proliferation, Proc. Natl. Acad. Sci. 88 (1991) 1883–1887.
[56] B. Eghbali, J. Kessler, L. Reid, C. Roy, D. Spray, Involvement of gap junctions in tumorigenesis: transfection of tumor cells with connexin32 cDNA retards growth in vivo, Proc. Natl. Acad. Sci. 88 (1991) 10701–10705.